Dalton Transactions

Anion-driven structures and SMM behavior of dinuclear terbium and ytterbium complexes

Journal:	*Dalton Transactions*
Manuscript ID	DT-ART-10-2018-004049.R1
Article Type:	Paper
Date Submitted by the Author:	15-Nov-2018
Complete List of Authors:	Mandal, Leena; Tohoku University, Department of Chemistry, Graduate School of Science BISWAS, SOUMAVA; Advanced Institute for Materials Research (WPI-AIMR), Tohoku University, Cosquer, Goulven; Tohoku University, Chemistry Shen, Yongbing; Tohoku University, Chemistry Yamashita, Masahiro; Tohoku University, Chemistry

SCHOLARONE™
Manuscripts

Please do not adjust margins

Journal Name

ARTICLE

Anion-driven structures and SMM behavior of dinuclear terbium and ytterbium complexes

Received 00th January 20xx,
Accepted 00th January 20xx

DOI: 10.1039/x0xx00000x

www.rsc.org/

Leena Mandal,[a] Soumava Biswas,*[b] Goulven Cosquer,[a] Yongbing Shen[a] and Masahiro Yamashita*[a,b,c]

The work in this present investigation reports the syntheses, crystal structures and magnetic properties of five dinuclear lanthanide complexes having composition $[Tb_2(HL)_4(NO_3)_6]$ (**1**), $[Tb_2(HL)_4Cl_6]\cdot 2EtOH$ (**2**), $[Yb_2(HL)_4(NO_3)_6]$ (**3**), $[Yb_2(HL)_4Cl_6]\cdot 2EtOH$ (**4**) and $[Y_2(HL)_4(NO_3)_6]$ (**5**) with HL = 8-hydroxyquinaldine. It is evident from the crystal structures, that, the coordination number of trivalent lanthanide ions in compounds **1**, **3** and **5** is nine, whereas, that for compounds **2** and **4** is six. Dynamic magnetic study shows that both compounds **1** and **3** exhibit single-molecule-magnet (SMM) behavior while compounds **2** and **4** do not have any SMM property.

Introduction

The increasing interest for the exploration of single molecule magnets (SMMs) is the foremost proof of their potential usefulness in quantum computing, high-density data storage, magnetic refrigeration, molecular spintronics and the fabrication of nanoscopic devices.[1,2] SMMs are a unique class of molecular materials, capable to block their magnetization for a long time, with a purely molecular origin.[3] The presence of their large spin ground state along with an intrinsic magnetic anisotropy leads to a high anisotropic energy barrier (Δ) for the reversal of magnetization. In particular, enormous effort has been devoted to design lanthanide-based SMMs in recent years because suitable lanthanide ions could exhibit unquenched orbital angular momentum and large intrinsic magnetic anisotropy as well as a large spin ground state. However, understanding the interference between magnetic exchange interaction and the origin of single ion anisotropy in lanthanide-based polynuclear systems are still a challenging task.[4] In this regard, dinuclear lanthanide SMMs could be very useful model systems to study the single-ion anisotropy and magnetic relaxation mechanism in molecules having high-nuclearity.[5] Beside this, the magnetic properties of dinuclear lanthanide SMMs can be tuned by changing several factors, like local coordination environment, bridging mode, functionalization of ligand *etc*.[5] $\{[(Me_3Si)_2N]_2Tb(THF)\}_2(\mu\text{–}\eta^2\text{:}\eta^2\text{-}N_2)^-$, one of the most exciting dinuclear SMM having blocking temperature 14 K, was reported so far by Long *et al*.[6] Also, they explored SMM behavior of a strongly exchange-coupled dinuclear dysprosium based SMM having high anisotropy barrier value.[6] $[hqH_2][Ln_2(hq)_4(NO_3)_3]\cdot MeOH$ (hqH = 8-hydroxyquinoline) is another nice example of dinuclear SMM where the direct magnetic exchange between two dysprosium(III) ions was investigated in details.[7] Up to now a variety of dinuclear lanthanide SMMs are documented in literature.[8–10]

8-hydroxyquinoline and its derivatives, because of their of flexible coordination modes, are very useful for the syntheses and magnetic study of versatile lanthanide-based complexes.[11–13] Beside this, ytterbium based molecular systems are very less explored in terms of their magnetic dynamics despite of the inherent magnetic anisotropy.[10a–d] So combination of 8-hydroxyquinoline and ytterbium ion could lead to prompting dinuclear model systems to study and compare with other analogous complexes. In this regard, 8-hydroxyquinaldine (HL) has been employed to construct five dinuclear lanthanide complexes with various lanthanide salts.

[a] Department of Chemistry, Graduate School of Science, Tohoku University, 6-3 Aza-Aoba, Aramaki, Sendai 980-8578, Japan.E-mail:yamasita.m@gmail.com
[b] WPI Research Center, Advanced Institute for Materials Research, Tohoku University, 2-1-1 Katahira, Aoba-ku, Sendai 980-8577, Japan, E-mail:biswassoumava@gmail.com
[c] School of Materials and Engineering, Nankai University, Tianjin 300350, China

†*Electronic Supplementary Information (ESI) available: Tables S1–S7 and Figs. S1–S10. CCDC 1871949–1871953 for* ***1–5****, respectively, contain the supplementary crystallographic data for this paper.*

This journal is © The Royal Society of Chemistry 20xx

Please do not adjust margins

Reactions of lanthanide nitrate salts with 8-hydroxyquinaldine afford three iso-structural nine coordinated dinuclear complexes showing field dependent SMM property for terbium and ytterbium complexes. Whereas, reactions of chloride salts give six coordinated dinuclear analogs, without any SMM behavior. The present work systematically explores, that, the effect of variation in the coordination environment of the lanthanide ion leads to a significant change in their molecular magnetic behaviour.

Experimental Section

Materials and physical measurements

All reagents and solvents were purchased from commercial sources and used as received. Elemental analyses (C, H and N) were performed at the Research and Analytical centre for Giant Molecules, Tohoku University. IR spectra of samples were acquired at room temperature with a JASCO FT/IR-4200 spectrophotometer. PXRD measurements were performed on a BRUKER D2 PHASER. Magnetic susceptibility measurements were conducted using a Quantum Design SQUID magnetometer MPMS-5S (Quantum Design, San Diego, CA, USA). AC measurements were performed with an ac field amplitude of 3 Oe. A polycrystalline sample embedded in *n*-eicosane was used for the measurements. EDX analysis was performed by an EDAX system equipped with a HITACHI S-4300 Scanning Electron Microscope.

Syntheses

$[Tb_2(HL)_4(NO_3)_6]$ (1). A methanol solution (5 ml) of $Tb(NO_3)_3{\cdot}6H_2O$ (0.091 g, 0.2 mmol) was added to a methanol solution (10 ml) of HL (0.080 g, 0.5 mmol). The mixture was stirred for 30 minutes and then filtered. The resulting brown solution was heated in a capped glass vial at 60 °C for four days. Yellow crystals suitable for X-Ray measurements were collected by filtration and washed with cold methanol. Yield (based on Tb): 0.050 g (38%). Anal. calcd for $C_{40}H_{36}N_{10}O_{22}Tb_2$: C, 36.21; H, 2.74; N, 10.56%. Found: C, 36.28; H, 2.94; N, 10.47%. IR (cm^{-1}): 3287(m), 3250(m), 3199(m), 1633(m), 1582(s), 1537(w), 1463(s), 1435(m), 1391(m), 1307(s), 1289(s), 1094(m), 1035(s), 891(m), 826(s) and 738(s).

$[Tb_2(HL)_4Cl_6]{\cdot}2EtOH$ (2). An ethanol solution (4 ml) of $TbCl_3{\cdot}6H_2O$ (0.149 g, 0.4 mmol) was added to a ethanol/acetonitrile (2:1) solution (6 ml) of HL (0.159 g, 1.0 mmol). The mixture was stirred for 30 minutes and then filtered. The resulting brown solution was heated in a capped glass vial at 60° C for four days. Yellow crystals suitable for X-Ray measurements were collected by filtration and washed with cold ethanol. Yield (based on Tb): 0.113 g (45%). Anal. calcd for $C_{44}H_{48}N_4O_6Cl_6Tb_2$: C, 41.96; H, 3.84; N, 4.45%. Found: C, 41.85; H, 4.04; N, 4.67%. IR (cm^{-1}): 3334(m), 3263(m), 3181(m), 1631(m), 1584(s), 1460(s), 1384(m), 1323(s), 1290(s), 1096(m), 1040(m), 925(w), 869(m), 822(s) and 741(s).

$[Yb_2(HL)_4(NO_3)_6]$ (3). This compound was prepared following the similar procedure to that described for **1** except using $Yb(NO_3)_3{\cdot}5H_2O$ (0.090 g, 0.2 mmol) instead of $Tb(NO_3)_3{\cdot}6H_2O$. Yield (based on Yb): 0.054g (40%). Anal. calcd for $C_{40}H_{36}N_{10}O_{22}Yb_2$: C, 35.46; H, 2.68; N, 10.34%. Found: C, 35.44; H, 2.77; N, 10.30%. IR (cm^{-1}): 3282(m), 3247(m), 3195(m), 1633(m), 1583(s), 1539(w), 1466(s), 1434(m), 1392(m), 1303(s), 1292(s), 1095(m), 1037(s), 894(m), 825(s) and 742(s).

$[Yb_2(HL)_4Cl_6]{\cdot}2EtOH$ (4). This compound was prepared following the similar procedure to that described for **2** except using $YbCl_3{\cdot}6H_2O$ (0.155 g, 0.4 mmol) instead of $TbCl_3{\cdot}6H_2O$. Yield (based on Yb): 0.121 g (47%). Anal. calcd for $C_{44}H_{48}N_4O_6Cl_6Yb_2$: C, 41.04; H, 3.76; N, 4.35%. Found: C, 40.81; H, 3.74; N, 4.49%. IR (cm^{-1}): 3352(m), 3267(m), 3154(m), 1632(m), 1585(s), 1461(s), 1383(m), 1325(s), 1291(s), 1098(m), 1042(m), 925(w), 869(m), 822(s) and 744(s).

$[Y_2(HL)_4(NO_3)_6]$ (5). This compound was prepared following the similar procedure to that described for **1** except using $Y(NO_3)_3{\cdot}6H_2O$ (0.077 g, 0.2 mmol) instead of $Tb(NO_3)_3{\cdot}6H_2O$. Yield (Based on Y): 0.050 g (42%). Anal. calcd for $C_{40}H_{36}N_{10}O_{22}Y_2$: C, 40.49; H, 3.06; N, 11.80%. Found: C, 40.54; H, 3.07; N, 11.84%. IR (cm^{-1}): 3286(w), 3249(m), 3197(m), 1633(m), 1583(s), 1537(w), 1464(s), 1434(m), 1391(m), 1302(s), 1290(s), 1095(m), 1036(s), 894(m), 824(s) and 739 (s).

$[(Y_{0.87}Tb_{0.13})_2(HL)_4(NO_3)_6]$ (1'). This compound was prepared following the similar procedure to that described for **1** except using $Y(NO_3)_3{\cdot}6H_2O$ (0.069 g, 0.18 mmol) and $Tb(NO_3)_3{\cdot}6H_2O$ (0.009 g, 0.02 mmol) instead of pure $Tb(NO_3)_3{\cdot}6H_2O$. The ratio of Y^{III} and Tb^{III} ions in complex was confirmed from elemental analysis, EDX spectrum and *χT vs. T* plot. (Fig. S1 and S2). Yield: 0.049 g (41%). Anal. calcd for $C_{40}H_{36}N_{10}O_{22}(Y_{0.87}Tb_{0.13})_2$: C, 39.88; H, 3.01; N, 11.63%. Found: C, 39.91; H, 3.08; N, 11.70%. IR (cm^{-1}): 3281(m), 3250(m), 3199(m), 1633(m), 1583(s), 1537(w), 1465(s), 1435(m), 1392(m), 1301(s), 1291(s), 1095(m), 1037(s), 893(m), 825(s) and 739(s).

Crystal structure determination

The crystallographic data are summarized in Table 1. Diffraction data were collected on a Rigaku Saturn 724+ CCD diffractometer with graphite monochromated Mo-Kα radiation (λ = 0.71073 Å). The data collection temperature was 100 K excepted for **2**, which was collected at 120 K. Data processing was performed using the CrystalClear crystallographic software package.[14] The structures were solved by SIR-92 [15] using direct methods and the structures were refined by full-matrix least-squares based on F^2 using SHELXL-2014/7[16] packages. Hydrogen atoms, linked with nitrogen atoms (N1 and N2) in **1**, **3** and **5** were located from difference Fourier maps. All other hydrogen atoms in **1**–**5** were placed at fixed geometrical positions and refined freely. The hydrogen

This journal is © The Royal Society of Chemistry 20xx

Table 1 Crystallographic data for **1**–**5**

	1	**2**	**3**	**4**	**5**
Empirical formula	$C_{40}H_{36}N_{10}O_{22}Tb_2$	$C_{44}H_{48}N_4O_6Cl_6Tb_2$	$C_{40}H_{36}N_{10}O_{22}Yb_2$	$C_{44}H_{48}N_4O_6Cl_6Yb_2$	$C_{40}H_{36}N_{10}O_{22}Y_2$
Formula weight	1326.63	1259.40	1354.87	1287.64	1186.61
Crystal system	Monoclinic	Monoclinic	Monoclinic	Monoclinic	Monoclinic
Space group	$P2_1/n$	$P2_1/c$	$P2_1/n$	$P2_1/c$	$P2_1/n$
a /Å	10.648(2)	10.835(5)	10.600(3)	10.793(4)	10.614(5)
b /Å	18.182(4)	12.142(6)	18.102(4)	12.085(4)	18.172(8)
c /Å	12.408(3)	18.646(9)	12.383(3)	18.496(6)	12.413(6)
α /°	90	90	90	90	90
β /°	110.205(3)	105.818(7)	110.001(3)	105.298(5)	110.223(5)
γ /°	90	90	90	90	90
V /Å^3	2254.4(9)	2360(2)	2232.8(10)	2327.0(14)	2246.6(18)
Z	2	2	2	2	2
ρ_{calcd} /g cm^{-3}	1.954	1.772	2.015	1.838	1.754
λ (Mo K$_\alpha$)/Å	0.71073	0.71073	0.71073	0.71073	0.71073
μ /mm^{-1}	3.211	3.362	4.263	4.390	2.670
T /K	100(2)	120(2)	100(2)	100(2)	100(2)
F(000)	1304	1240	1324	1260	1200
2ϑ range for data collection /°	8.006–54.966	8.106–54.962	8.044–54.972	8.146–50.484	8.022–54.980
Index ranges	$-13 \le h \le 13$	$-14 \le h \le 11$	$-8 \le h \le 13$	$-13 \le h \le 13$	$-13 \le h \le 13$
	$-23 \le k \le 23$	$-15 \le k \le 9$	$-15 \le k \le 22$	$-14 \le k \le 11$	$-17 \le k \le 23$
	$-15 \le l \le 16$	$-24 \le l \le 23$	$-16 \le l \le 15$	$-22 \le l \le 15$	$-15 \le l \le 10$
No. measured reflections	18090	11123	8887	8341	9088
No. independent reflections	5109	5331	5008	4527	5086
R_{int}	0.0496	0.1026	0.0431	0.0479	0.0723
No. refined parameters	344	224	344	206	344
No. observed reflections, $I > 2\sigma(I)$	4217	3110	3485	3199	3096
Goodness-of-fit on F^2, S	0.999	0.913	1.006	1.058	1.027
R_1^a, wR_2^b [$I > 2\sigma(I)$]	0.0353, 0.0708	0.0787, 0.1682	0.0316, 0.0640	0.0575, 0.1350	0.0668, 0.1002
R_1^a, wR_2^b (all data)	0.0482, 0.0767	0.1379, 0.2197	0.0452, 0.0675	0.0874, 0.1602	0.1318, 0.1179

$^aR_1 = [\sum||F_o| - |F_c||/\sum|F_o|]$. $^bwR_2 = [\sum w(F_o^2 - F_c^2)^2/\sum w(F_o^2)^2]^{1/2}$

atoms were refined isotropically, while the non-hydrogen atoms were refined anisotropically.

Results and discussion

Syntheses and characterization

Compounds **1**, **3** and **5** were prepared by the reaction of HL and Ln-nitrate salt in 5:2 molar ratio in methanol at 60 °C. Compounds **2** and **4** were prepared by the reaction of HL and Ln-chloride salt in 5:2 molar ratio in ethanol/acetonitrile at 60 °C. These complexes were synthesized by the similar methods done for the previously reported dysprosium and gadolinium analogs.[13] Furthermore, the powder X-ray diffraction pattern (PXRD) of the synthesized samples matched well with the simulated pattern for the single crystal data, which confirmed the phase purity of bulk sample (Fig. S3).

Description of crystal structures

Compounds **1**, **3** and **5** are iso-structural and crystallize in the monoclinic space group $P2_1/n$ (Fig. 1a). Selected bond lengths and bond angles in the coordination environment of the trivalent lanthanide ions are listed in Table S1. The centro-symmetric structures consist of two Ln^{III} ions, six nitrate

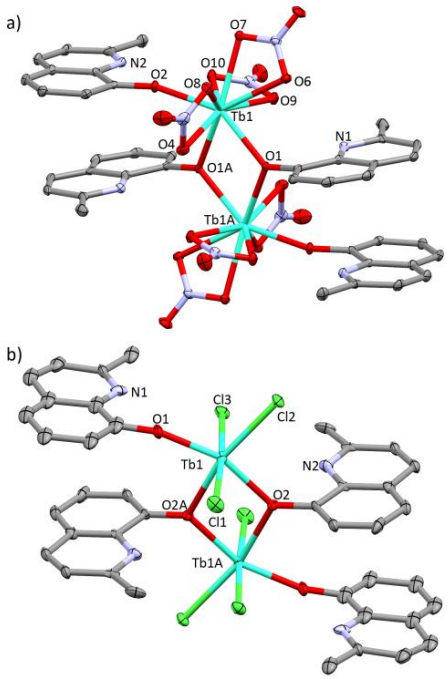

Fig.1 Crystal structure of a) **1** and b) **2**. Hydrogen atoms for **1** and **2** and solvent ethanol molecule for **2** are omitted for clarity. Symmetry code: *A, 2–x, 1–y, 1–z* for **1** and A, *–x, 2–y, –z for* **2**.

moieties and four HL ligands. The lanthanide ions are diphenoxo-bridged and nine-coordinated with a distorted spherical capped square antiprism coordination geometry, determined by SHAPE 2.1[17] (Table S2). Six coordination positions are satisfied by oxygen atoms from the nitrate moieties, and the three remaining coordination sites are occupied $O_{phenoxo}$ atoms of three HL ligands, with two μ_2 and one μ_1 coordination mode. As, the HL ligands, coordinated to each lanthanide ion, have deprotonated phenoxo oxygen atoms and protonated quinoline nitrogen atoms, the +III charge of each lanthanide ion of the neutral dinuclear core is balanced by the three coordinated nitrate anions.

Compounds **2** and **4** are also iso-structural and consist of neutral, centro-symmetric dinuclear core. They crystallize in monoclinic space group $P2_1/c$ (Fig. 1b and Table S3). Unlike **1**, **3** and **5** the lanthanide centres are hexa-coordinated and have a distorted octahedron geometry (Table S4). Each Ln^{III} centre is coordinated to $O_{phenoxo}$ atoms of three HL ligands, with two μ_2 and one μ_1 coordination mode. The other three coordination positions are satisfied by three chloride ions. The +III charge of each lanthanide ion is balanced by these coordinated chloride ions as the coordinated HL ligands are neutral.

Intramolecular $Ln^{III}\cdots Ln^{III}$ separation is 3.928(1), 3.846(2), 3.831(1), 3.728(1) and 3.884(2) Å for **1–5**, respectively. The intermolecular $Ln^{III}\cdots Ln^{III}$ separation is more than 9.3 Å for the compounds **1–5**. There are intramolecular and intermolecular π···π stacking interactions between the HL moieties in compounds **1–5** (Fig. S4 and S5). The intramolecular π···π stacking distances lie in the range 3.344–3.673 Å, for **1**, **3** and **5** and 3.913–4.023 Å for **2** and **4**, respectively. The range of intermolecular π···π stacking distances for **1–5** is 3.661–3.784 Å.

Magnetic Properties

Direct current (dc) magnetic susceptibility measurements for polycrystalline samples were performed in the temperature range of 2–300 K at 1000 Oe (Fig. 2).

The room temperature χT values of 23.79 and 24.17 $cm^3\cdot K\cdot mol^{-1}$ have been observed for **1** and **2**, respectively. This value agrees with the expected value of 23.63 $cm^3\cdot mol^{-1}\cdot K$ ($^7F_6$, g = 3/2) for two uncoupled Tb^{III} ions at 300 K. For complex **1**, the χT values decrease gradually with the decrease of the temperature to 20.17 $cm^3\cdot mol^{-1}\cdot K$ at 9 K. This initial decrease in χT values may be due to the thermal depopulation of the m_J sublevels.[18] Below 9 K, the steep rise of χT indicates the presence of ferromagnetic interaction at low temperature.[19] In complex **2**, the χT values continuously decrease with an acceleration below 23 K to reach the value of 6.11 $cm^3\cdot mol^{-1}\cdot K$ at 2 K. This behavior suggests antiferromagnetic interaction or depopulation of the m_J sublevels.

For complex **3,** the room temperature χT value of 5.36 $cm^3\cdot mol^{-1}\cdot K$ is consistent with two uncoupled Yb^{III} ions (5.14 $cm^3\cdot mol^{-1}\cdot K$, $^2F_{7/2}$, g = 8/7). With the decrease in temperature,

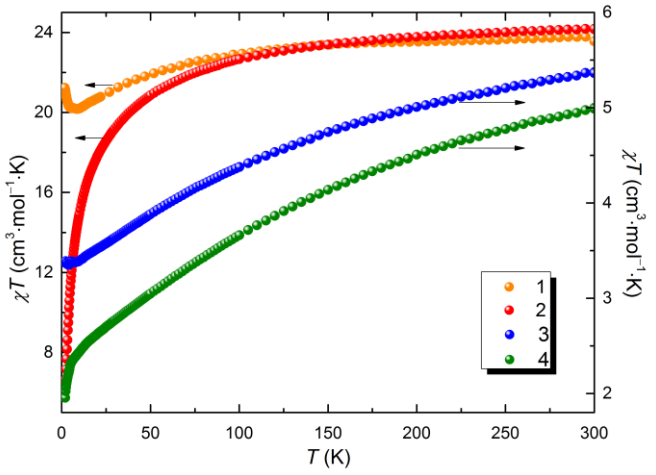

Fig. 2 Temperature dependence of the χT *vs.* *T* in 1000 Oe field for complexes **1-4**.

the χT value decreases to a value of 3.37 $cm^3\cdot mol^{-1}\cdot K$ around 7 K by depopulation of m_J sublevels. Further small increase in χT below 4 K suggests the presence of small ferromagnetic interactions. In complex **4**, χT value decreases gradually from room temperature (4.99 $cm^3\cdot mol^{-1}\cdot K$) to a 2.31 $cm^3\cdot mol^{-1}\cdot K$ at around 5 K. After that, a sharp decrease was observed. None of the complexes show hysteresis in isothermal magnetization measurements. The non-saturation of the magnetization at 5 T indicates the presence of magnetic anisotropy and/or low-lying excited states (Fig S6).

To investigate the magnetic dynamics, ac magnetic susceptibility measurements were carried out for **1–4**. In absence of any external dc magnetic field, no frequency dependence was observed (Fig. S7), which can be attributed to a fast quantum tunnelling of the magnetization (QTM).[20] To suppress this QTM, ac magnetic susceptibility measurements were performed in an optimized dc magnetic field (Fig. S8). For complex **1**, an optimized dc field of 3000 Oe was applied (Fig. 3). As a result, a multi-peak maxima were observed in the out-of-phase ac susceptibility data as a function of frequency. The presence of a multi-peak may be due to inter- or intra-molecular exchange or dipolar interactions.[21] The presence of merged multi-peak prevents us to be able to extract relaxation times by fitting the experimental data.

In order to determine the origin of the multiple relaxation time, a magnetically diluted sample, **1'**, with a Tb^{III}:Y^{III} ratio of 1:9 was synthesized. For **1'**, at an optimized applied field of 1600 Oe, a single peak maxima were observed in the out-of-phase signal (Fig. S9). The relaxation time for **1'** has been obtained from the fitting of the experimental data by using the Cole-Cole model (Fig. S10 and Table S5).[22] Nevertheless, relaxation time at the lowest temperature is close to the equipment limit, which make difficult the determination of the relaxation process. The obtained process, combination of direct and Raman, are subject to caution (Fig. 4 and Table 2). In this case, equation (1) has been used.[4a]

$$\tau^{-1} = AH^4T^n + CT^m \qquad (1)$$

This journal is © The Royal Society of Chemistry 20xx

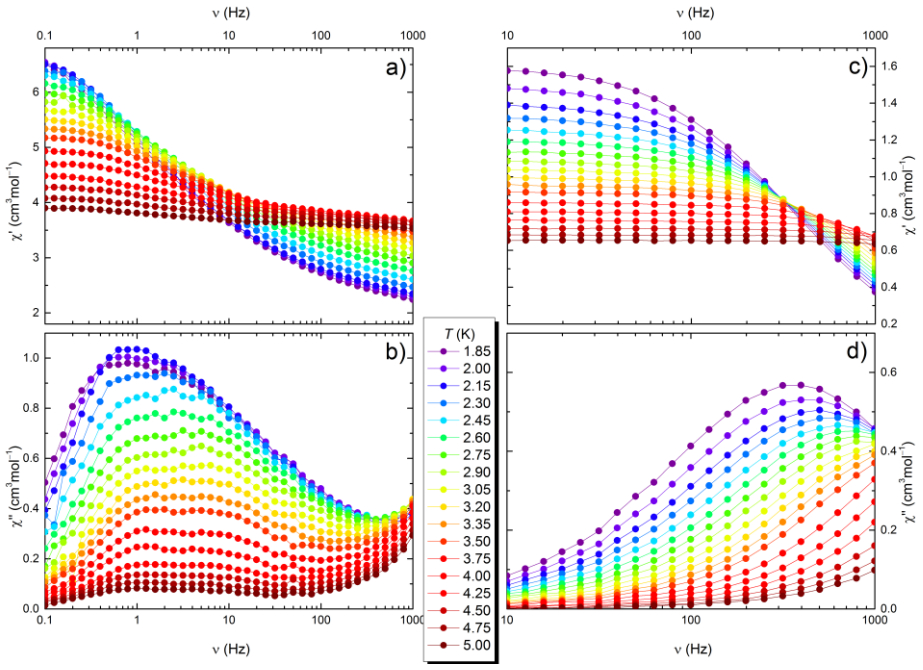

Fig. 3 Frequency dependence of the in phase (a and c) and out of phase (b and d) components of the ac magnetic susceptibility for **1** (a and b) and **3** (c and d), under 3000 Oe dc field.

In complex **3**, for an applied optimized field of 3000 Oe, frequency dependent peak maxima were found (Fig. 3). This observation confirms the presence of slow magnetic relaxation as well as field-induced single molecule magnetic behavior,[23] which, in case of ytterbium complexes is rare in nature.[10a–d,24] The ac susceptibility data were fitted with the Cole-Cole model for the temperature range of 1.8–2.9 K (Fig. S10 and Table S6). Similarly to **1'**, the relaxation time of **3** is close to the limit of our equipment and make difficult the determination of the relaxation process. The obtained process (Orbach) are subject to caution (Fig. 4 and Table 2). The parameters in Table 2 have been obtained using equation (2).[4a]

$$\tau^{-1} = \tau_0^{-1}\exp(-\Delta/k_BT) \qquad (2)$$

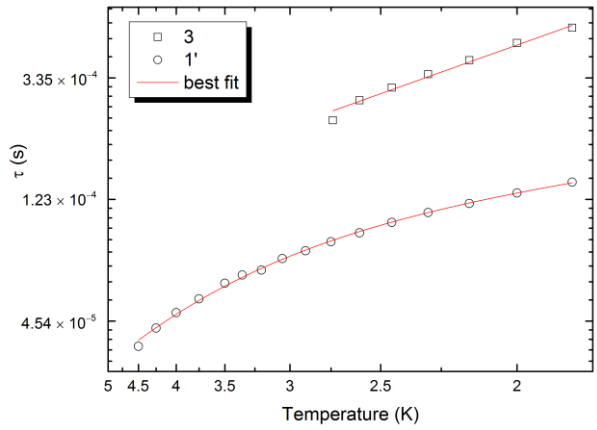

Fig. 4 Temperature dependence of relaxation time.

Table 2 List of parameters related to magnetic properties of **1'** and **3**

Parameter	Unit	Complex **1'**	Complex **3**
A	$s^{-1}H^{-4}K^{-2}$	5.56×10^{-10}	–
H	Oe	1600	–
n	–	1	–
Δ	cm^{-1}	–	2.78
τ_0	s	–	5.93×10^{-5}
C	$s^{-1}K^{-m}$	24.26	–
m	–	4	–

So for this ytterbium complex, the resultant energy barrier and magnetic relaxation time are quite consistent with other similar ytterbium based SMMs (Table S7); for example $[Yb_2L_2(acac)_2(H_2O)]\cdot2CH_2Cl_2$ shows field induced SMM behavior.[10b] Whereas, a single magnetic relaxation was observed for $[Yb_2(DBM)_6(L)]$ at an applied field of 2000 Oe.[10a] Similarly, a binuclear complex, $[Yb(dnbz)(acac)_2(H_2O)(EtOH)]_2$ exhibits field dependent SMM character having an energy barrier of 26K.[10c]

For **2** and **4**, no effect dc field on magnetic relaxation was obtained, which confirms the non SMM nature of these two complexes (Fig. S8).[25]

Now, from the magneto-structural correlation, it is obvious that the coordination geometry around the lanthanide centres are directly affecting the magnetic dynamics for the complexes. It is found that the deviation from a spherical symmetry (like cubic) generates more crystal-field (CF) splitting.[26] In this case, the hexa-coordinated (octahedral) lanthanide centres are quite close to a

spherical environment. So lack of crystal-field (CF) splitting leads to the non-SMM behavior for hexa-coordinated complexes. Whereas for the nine coordinated, distortion from spherical symmetry is comparatively high which enhances the crystal-field (CF) effects as well as the SMM properties.[26]

Conclusions

Five 8-hydroxyquinaldine based lanthanide (Ln = Tb, Yb and Y) complexes have been explored in terms of their structural features and magnetic properties. Controlled change of counter anions of lanthanide salts in reaction condition leads to two different complexes in terms of coordination geometry of the metal ion. Both static (dc) and dynamic (ac) magnetic properties have been investigated thoroughly for all the complexes. Notably, at low-temperature ferromagnetic exchange interaction is observed for complexes using NO_3^- as counter ion, but antiferromagnetic interaction for Cl^- ones. Both NO_3^- coordinated complexes show field induced SMM behavior. Specifically, complex **3** is a rare example of ytterbium based SMM. Contrarily, SMM behavior has completely vanished for the Cl^- coordinated analogs. So the use of 8-hydroxyquinoline based ligand with a systematic change in reaction medium is a beneficial strategy to prepare lanthanide complexes with different magnetic properties. In the field of lanthanide-based SMMs, such complexes could be useful for the understanding of structure–property relationship.

Conflicts of interest

There are no conflicts to declare.

Acknowledgements

This work was partially supported by CREST (JPMJCR12L3), JST. M. Yamashita thanks the supports by 111 project (B18030) from China. S.B. thanks JSPS for financial support.

References

1 (*a*) B. Sieklucka and D. Pinkowicz, Molecular Magnetic Material: Concepts and Applications; Wiley–VCH:, Wienheim, 2017; (*b*) M. N. Leuenberger and Daniel Loss, *Nature*, 2001, **410**, 789; (*c*) M. Urdampilleta, S. Klyatskaya, J.-P. Cleuziou, M. Ruben and W.Wernsdorfer, *Nat. Mater,* 2011, **10**, 502; (*d*) L. Bogani and W. Wernsdorfer, *Nat. Mater*., 2008, **7**, 179; (*e*) A. Cornia, M. Mannini, P. Sainctavitc and R. Sessoli, *Chem. Soc. Rev.*, 2011, **40**, 3076.

2 S. Biswas, A. K. Mondal and S. Konar, *Inorg. Chem*., 2016, **55**, 2085.

3 (*a*) D. N. Woodruff, R. E. P. Winpenny and R. A. Layfield, *Chem. Rev.*, 2013, **113**, 5110; (*b*) K. Katoh, B. K. Breedlove and M. Yamashita, *Chem*. *Sci*., 2016, **7**, 4329; (*c*) D. Gatteschi, R. Sessoli and J. Villain, *Molecular Nanomagnets*, Oxford University Press, Oxford, U.K., 2006; (*d*) D. Gatteschi and R. Sessoli, *Angew. Chem. Int. Ed*., 2003, **42**, 268; (*e*) S. Mandal, S. Mondal, C. Rajnák, J. Titiš, R. Boča and S. Mohanta, *Dalton Trans*., 2017, **46**, 13135; (*f*) S. Ghosh, S. Mandal, M. K. Singh, C.-M. Liu, G. Rajaraman and S. Mohanta, *Dalton Trans*., 2018, **47**, 836.

4 (*a*) S. T. Liddle and J. v. Slageren, *Chem*. *Soc*. *Rev*., 2015, **44**, 6655; (*b*) L. Sorace, C. Benelli and D. Gatteschi, *Chem*. *Soc*. *Rev*., 2011, **40**, 3092.

5 (*a*) T. Morita, M. Damjanović, K. Katoh, Y. Kitagawa, N. Yasuda, Y. Lan, W. Wernsdorfer, B. K. Breedlove, M. Enders and M. Yamashita, *J*. *Am*. *Chem*. *Soc*., 2018, **140**, 2995; (*b*) F. Habib and M. Murugesu, *Chem. Soc. Rev.,* 2013, **42**, 3278.

6 (*a*) J. D. Rinehart, M. Fang, W. J. Evans and J. R. Long, *J*. *Am*. *Chem*. *Soc*., 2011, **133**, 14236; (*b*) J. D. Rinehart, M. Fang, W. J. Evans, J. R. Long, *Nat*. *Chem*., 2011, **3**, 538.

7 E. M. Pineda, N. F. Chilton, R. Marx, M. Dorfel, D. O. Sells, P. Neugebauer, S.-D. Jiang, D. Collison, J. V. Slageren, E. J.L. McInnes, R. E. P. Winpenny, *Nat. Commun*., 2014, **5**, 5243.

8 (*a*) W.-M. Wang, W.-W. Duan, L.-C. Yue, Y.-L. Wang, W.-Y. Ji, C.-F. Zhang, M. Fang and Z.-L. Wu, *Inorg*. *Chim*. *Acta*, 2017, **466**, 145; (*b*) S. Sakaue, A. Fuyuhiro, T. Fukuda and N. Ishikawa, *Chem*. *Commun*., 2012, **48**, 5337; (*c*) J. Vallejo, J. Cano, I. Castro, M. Julve, F. Lloret, O. Fabelo, L. Cañadillas-Delgado and E. Pardo, *Chem*. *Commun*., 2012, **48**, 7726; (*d*) H. Sun, L. Wu, W. Yuan, J. Zhao and Y. Liu, *Inorg*. *Chem*. *Commun*., 2016, **70**, 164; (*e*) Y.-B. Lu, X.-M. Jiang, S.-D. Zhu, Z.-Y. Du, C.-M. Liu, Y.-R. Xie and L.-X. Liu, *Inorg*. *Chem*., 2016, **55**, 3738.

9 (*a*) L. Zhao, J. Wu, H. Ke and J. Tang, *CrystEngComm*, 2013, **15**, 5301; (*b*) W.-B. Sun, B.-L. Han, P.-H. Lin, H.-F. Li, P. Chen, Y.-M. Tian, M. Murugesu and P.-F. Yan, *Dalton Trans*., 2013, **42**, 13397; (*c*) A. K. Mondal, V. S. Parmar and S. Konar, *Magnetochemistry*, 2016, **2**, 35; (*d*) X.-L. Li, C.-L. Chen, Y.-Li. Gao, C.-M. Liu, X.-Li. Feng, Y.-H. Gui and S.-M. Fang, *Chem*. *Eur*. *J*., 2012, **18**, 14632; (*e*) M. Nematirad, W. J. Gee, S. K. Langley, N. F. Chilton, B. Moubaraki, K. S. Murray and S. R. Batten, *Dalton Trans*., 2012, **41**, 13711.

10 (*a*) O. Sun, P. Chen, H.-F. Li, T. Gao, W.-B. Sun, G.-M. Li and P.-F. Yan, *CrystEngComm*, 2016, **18**, 4627; (*b*) P.-H. Lin, W.-B. Sun, Y.-M. Tian, P.-F. Yan, L. Ungur, L. F. Chibotaru and M. Murugesu, *Dalton Trans*., 2012, **41**, 12349; (*c*) A. V. Gavrikov, N. N. Efimov, A. B. Ilyukhin, Z. V. Dobrokhotovaand and V. M. Novotortsev, *Dalton Trans*., 2018, **47**, 6199; (*d*) T.-Q. Liu, P.-F. Yan, F. Luan, Y.-X. Li, J.-W. Sun, C. Chen, F. Yang, H. Chen, X.-Y. Zou and G.-M. Li, *Inorg*. *Chem*., 2015, **54**, 221; (*e*) Y. Qin, H. Zhang, H. Sun, Y. Pan, Y. Ge, Y. Li and Y.-Q. Zhang, *Chem*. *Asian J*., 2017, **12**, 2834; (*f*) H. Zhang, S.-Y. Lin, S. Xue, C. Wang and J. Tang, *Dalton Trans*., 2014, **43**, 6262; (*g*) W.-M. Wang, X.-Y. Zhao, H. Qiao, L. Bai, H.-F. Hana, M. Fang, Z.-L. Wu and J.-Y. Zou, *J*. *Solid State Chem*., 2017, **253**, 154; (*h*) I. F. Díaz-Ortega, J. M. Herrera, D. Aravena, E. Ruiz, T. Gupta, G. Rajaraman, H. Nojiri and E. Colacio, *Inorg*. *Chem*., 2018, **57**, 6362.

11 (*a*) N. F. Chilton, G. B. Deacon, O. Gazukin, P. C. Junk, B. Kersting, S. K. Langley, B. Moubaraki, K. S. Murray, F. Schleife, M. Shome, D. R. Turner and J. A. Walker, *Inorg. Chem*., 2014, **53**, 2528; (*b*) D. Zhang, Y.-M. Tian, W.-B. Sun, H.-F. Li, P. Chen, Y.-Q. Zhang and P.-F. Yan, *Dalton Trans*., 2016, **45**, 2674; (*c*) W.-Y. Zhang, Y.-M. Tian, H.-F. Li, P. Chen, W.-B. Sun, Y.-Q. Zhang and P.-F. Yan, *Dalton Trans*., 2016, **45**, 3863.

12 H.-B. Xu, J. Li, L.-Y. Zhang, X. Huang, B. Li and Z. N. Chen, *Cryst. Growth Des.*, 2010, **10**, 4101.

13 F. Yang, Q. Zhou, G. Zeng, G. Li, L. Gao, Z. Shi and S. Feng, *Dalton Trans*., 2014, **43**, 1238.

14 Crystal Clear-SM, 1.4.0 SP1; Rigaku Corporation: Tokyo, Japan, 17 April 2008.

 This journal is © The Royal Society of Chemistry 20xx

15 A. Altomare, M. C. Burla, M. Camalli, G. L. Cascarano, C. Giacovazzo, A. Guagliardi, A. G. G. Moliterni, G. Polidori and R. Spagna, SIR97: A new tool for crystal structure determination and refinement, *J. Appl. Crystallogr*. 1999, **32**, 115.
16 G. M. Sheldrick, SHELXL-2014/7, Crystal Structure Refinement Program, University of Göttingen, 2014.
17 (*a*) S. Alvarez, P. Alemany, D. Casanova, J. Cirera, M. Llunell and D. Avnir, *Coord. Chem. Rev.*, 2005, **249**, 1693; (*b*) J. Cirera, E. Ruiz and S. Alvarez, *Chem. Eur. J.*, 2006, **12**, 3162.
18 (*a*) P. P. Yang, X. F. Gao, H. B. Song, S. Zhang, X. L. Mei, L. C. Li and D. Z. Liao, *Inorg. Chem*., 2011, **50**, 720; (*b*) Y. J. Gao, G. F. Xu, L. Zhao, J. K. Tang and Z. L. Liu, *Inorg. Chem*., 2009, **48**, 11495; (*c*) Y. N. Guo, G. F. Xu, W. Wernsdorfer, L. Ungur, Y. Guo, J. Tang, H. J. Zhang, L. F. Chibotaru and A. K. Powell, *J. Am. Chem. Soc*., 2011, **133**, 11948; (*d*) S. Biswas, H. S. Jena, S. Sanda and S. Konar, *Chem. Eur. J.*, 2015, **21**, 13793.
19 (*a*) S. Shen, S. Xue, S.-Y. Lin, L. Zhao and J. Tang, Dalton Trans., 2013, **42**, 10413; (*b*) T. Kanetomo, S. Yoshii, H. Nojiri and T. Ishida, *Inorg. Chem. Front*., 2015, **2**, 860; (*c*) Z. Chen, B. Zhao, P. Cheng, X. Q. Zhao, W. Shi and Y. Song, *Inorg. Chem*., 2009, **48**, 3493.
20 (*a*) M. Jeletic, P.-H. Lin, J. Le Roy, I. Korobkov, S. I. Gorelsky and M. Murugesu, *J. Am. Chem. Soc*., 2011, **133**, 19286; (*b*) F. Habib, P.-H. Lin, J. Long, I. Korobkov, W. Wernsdorfer and M. Murugeshu, *J. Am. Chem. Soc*., 2011, **133**, 8830.
21 (*a*) T. Morita, K. Katoh, B. K. Breedlove and M. Yamashita, *Inorg. Chem*., 2013, **52**, 13555; (*b*) R. J. Blagg, L. Ungur, F. Tuna, J. Speak, P. Comar, D. Collison, W. Wernsdorfer, E. J. L. McInnes, L. F. Chibotaru and R. E. P. Winpenny, *Nat. Chem*., 2013, **5**, 673.
22 Z. Liang, M. Damjanovic, M. Kamila, G. Cosquer, B. K. Breedlove, M. Enders and M. Yamashita, *Inorg. Chem*., 2017, **56**, 6512.
23 (*a*) M.-E. Boulon, G. Cucinotta, J. Luzon, C. Degl'Innocenti, M. Perfetti, K. Bernot, G. Calvez, A. Caneschi, and R. Sessoli, *Angew. Chem. Int. Ed*., 2013, **52**, 350; (*b*) M. Sugita, N. Ishikawa, T. Ishikawa, S.-Y. Koshihara and Y. Kaizu, *Inorg. Chem*., 2006, **45**, 1299.
24 A. B. Castro, J. Jung, S. Golhen, B. L. Guennic, L. Ouahab, O. Cador and F. Pointillart, *Magnetochemistry*, 2016, **2**, 26.
25 B. Na, X.-J. Zhang, W. Shi, Y.-Q. Zhang, B.-W. Wang, C. Gao, S. Gao and P. Cheng, *Chem. Eur. J.*, 2014, **20**, 15975.
26 M. Guo and J. Tang, *Inorganics*, 2018, **6**, 16.

Graphical Abstract

for

Anion-driven structures and SMM behavior of dinuclear terbium and ytterbium complexes

Leena Mandal, Soumava Biswas,* Goulven Cosquer, Yongbing Shen and Masahiro Yamashita*

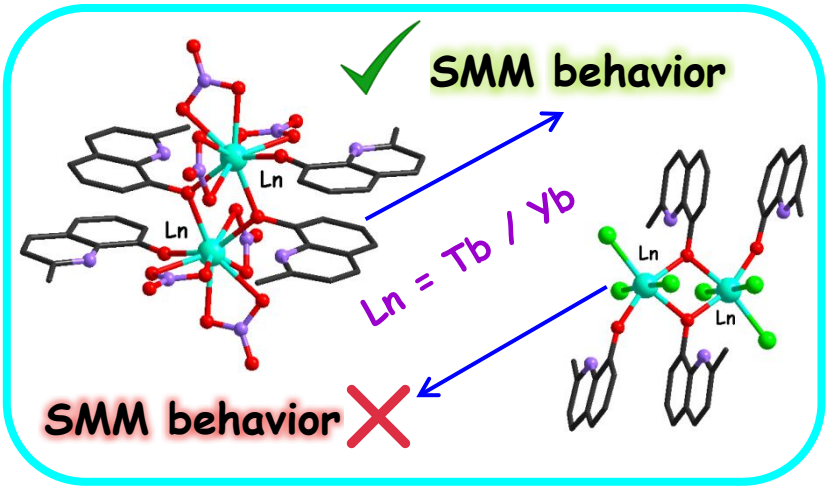

The present report deals with syntheses, crystal structures and magnetic properties of five dinuclear lanthanide complexes having composition $[Tb_2(HL)_4(NO_3)_6]$ (**1**), $[Tb_2(HL)_4Cl_6]\cdot 2EtOH$ (**2**), $[Yb_2(HL)_4(NO_3)_6]$ (**3**), $[Yb_2(HL)_4Cl_6]\cdot 2EtOH$ (**4**) and $[Y_2(HL)_4(NO_3)_6]$ (**5**) with HL = 8-hydroxyquinaldine. The coordination number of the lanthanide centres in **1** and **3** is nine and these complexes exhibit single-molecule-magnet (SMM) behavior. On the other hand, **2** and **4**, having hexa-coordinated lanthanide centres, do not show any SMM property.